# Hyperfine structure of $Na_2$

P. E. Van Esbroeck, R. A. McLean, T. D. Gaily, R. A. Holt, and S. D. Rosner
*Department of Physics, The University of Western Ontario, London, Ontario, Canada N6A 3K7*
(Received 1 July 1985)

The hyperfine structure has been measured in several rotational states of the $X^1\Sigma_g^+$, $v''=0$ ground state of $Na_2$ with the aid of the laser-rf double-resonance technique on a molecular beam. The rotational states observed were especially chosen to avoid distortion of the line shapes by laser-induced coherence effects. The electric quadrupole, nuclear spin-rotation, tensor spin-spin, and scalar spin-spin hyperfine coupling constants are, respectively, $eqQ=[-458.98(4)-0.007\,28(25)J(J+1)]$ kHz, $c=242.9(1.5)$ Hz, $d=302.6(5.0)$ Hz, and $\delta=1066.7(6.5)$ Hz.

## I. INTRODUCTION

The alkali-metal dimer molecules present an interesting challenge to the molecular physicist. Their resemblance to $H_2$ makes them attractive candidates for *ab initio* calculations, although they differ from $H_2$ in significant aspects such as the size of the binding energy of the neutral dimer relative to the dimer ion.[1] Because they are readily produced and have electronic states easily accessible with visible light, their gross and fine structure can be studied in great detail. The observation of lasing in $Na_2$ has generated a large number of experimental and theoretical investigations of these molecules in the past several years.[2] Their visible and ultraviolet systems have been mapped with unprecedented precision using various laser spectroscopic techniques;[3–10] lifetimes and Franck-Condon factors have been measured,[11,12] and triplet states have been observed through perturbations.[13,14] In response to this experimental activity, there have been several pseudopotential and *ab initio* calculations of electronic structure, yielding potential curves, dissociation energies,[15,16] transition dipole moments, and lifetimes.[17]

In addition to these studies of gross structure, there has also been significant activity in the measurement of hyperfine structure (hfs) in the sodium dimer, mainly using new laser techniques. Some information about the hfs and magnetic moments of the alkali-metal dimers has been available for years from conventional Rabi molecular-beam experiments.[18,19] The nuclear and rotational magnetic moments are known fairly precisely, whereas the values of the electric quadrupole coupling constants of the $^1\Sigma_g^+$ ground state have been rather crudely inferred from their effects on the line shape of nuclear spin-flip resonances involving many rotational levels simultaneously. In 1975, three of the present authors introduced a laser-rf double-resonance technique in which the hfs of a single rotational level could be observed directly, with a linewidth limited only by transit-time effects.[20] This work yielded the first measurement of the spin-rotation coupling constant $c$ and a more precise value for the quadrupole coupling constant $eqQ$. Later, Huber *et al.*[21] published NMR studies of alkali-metal dimers which used atom-molecule exchange in an optically pumped vapor; they used their values of magnetic shielding parameters to estimate $c$. In 1982, Atkinson *et al.*[14] resolved the hfs of the $a^3\Pi_u$ state using laser excitation of a supersonic molecular beam.

Further work in our laboratory[22] on the laser-rf double-resonance method showed that state selection and detection by strong optical fields can produce magnetic resonance line shapes which differ drastically from the Rabi shape, even though the optical and rf fields do not act simultaneously on the molecules. This behavior was attributed to the creation of coherence among ground-state hyperfine levels by the laser optical pumping cycle of absorption and stimulated emission. A model based on this idea reproduced the main features of the magnetic resonance line shapes, but there remained some notable discrepancies both in lines displaying obvious coherence effects and in those with apparently more conventional shapes.

Our original study of $Na_2$ hfs concentrated (because of available laser wavelengths) on the $v''=0$, $J''=28$, $X^1\Sigma_g^+$ state, which contains 342 magnetic sublevels. For computational reasons, it was necessary to limit the number of levels included in the model to those few believed to contribute most significantly to the observed signal. Because of the discrepancies referred to above, a new study was undertaken, this time of the $v''=0$, $J''=2$, $X^1\Sigma_g^+$ level.[23] This work confirmed the basic idea of the coherence model and led us to conclude that remaining discrepancies between experiment and model were primarily due to the omission of important interaction terms from the hfs model, rather than the neglect of magnetic sublevels or other computational approximations.

The double-resonance line shapes calculated from the model contain interference terms with factors of the form $\exp(i\Omega t)$, where $\Omega$ is a hyperfine interval and $t$ is the transit time of a molecule through the rf magnetic field region. The signal must be averaged over the velocity distribution of the molecular beam with the result that, for our experimental conditions, the exponential factors become negligible unless $\Omega/2\pi<20$ kHz. This implies that the anomalous line shapes should occur in a rf transition for which either the upper or lower hyperfine level is coherently mixed with a third hyperfine level which lies only a few kilohertz away. Thus, the effect of very small hyperfine interactions on level separations becomes enormously magnified in the line shape of these transitions.

 

Prompted by these considerations and the intrinsic interest in *ab initio* calculation of molecular hfs, we undertook a new measurement of the hfs of $Na_2$ using the laser-rf double-resonance method of our earlier work. In order to make the measurement virtually independent of coherence effects, we selected hyperfine transitions between pairs of levels both of which are far from other hyperfine levels to which they might be coupled by the light. Ultimately, we hope to use the measured hyperfine constants to refine our lineshape models to the point of complete quantitative agreement.

## II. THEORY

### A. Hyperfine structure

Beginning with the pioneering work of Frosch and Foley,[24] the theory of hyperfine structure in diatomic molecules has grown to include the effects of higher multipoles and has been recast in terms of irreducible tensor operators. Broyer *et al.*[25] have constructed an effective hyperfine Hamiltonian which takes into account all multipoles up to E4; they give a detailed account of all terms to second order in the hyperfine operators and the off-diagonal part of the molecular Hamiltonian which does not contain the nuclear spin (the rotation-electronic and electronic spin-orbit operators). For the $^1\Sigma_g^+$ ground state of $Na_2$, the leading term is the electric quadrupole (E2) interaction of the order of a few hundred kilohertz. Much smaller ($\sim$1 kHz), but still very significant to our precision, are the direct (first-order) and electron-coupled (second-order) magnetic interactions between the two nuclei. The complete matrix element of the *effective* Hamiltonian, including all these interactions is given by

$$\langle {}^1\Sigma_g^+ I''JF \,|\, H_{\rm hf} \,|\, {}^1\Sigma_g^+ IJF\rangle = \tfrac{1}{2}eqQ(-1)^{2I_1+F}\left[\frac{(2I_1+3)(2I_1+2)(2I_1+1)}{2I_1(2I_1-1)}\right]^{1/2}$$
$$\times[(2I+1)(2I''+1)]^{1/2}(2J+1)\begin{bmatrix} J & 2 & J \\ 0 & 0 & 0\end{bmatrix}\begin{Bmatrix} 2 & I_1 & I_1 \\ I_1 & I'' & I\end{Bmatrix}\begin{Bmatrix} F & J & I \\ 2 & I'' & J\end{Bmatrix}$$
$$+\frac{c}{2}[F(F+1)-I(I+1)-J(J+1)]\delta_{I'',I}+\frac{\delta}{2}[I(I+1)-2I_1(I_1+1)]\delta_{I'',I}$$
$$+d(-1)^{I''+F+1}[I_1(I_1+1)(2I_1+1)][30(2I+1)(2I''+1)]^{1/2}(2J+1)$$
$$\times\begin{bmatrix} J & 2 & J \\ 0 & 0 & 0\end{bmatrix}\begin{Bmatrix} F & J & I \\ 2 & I'' & J\end{Bmatrix}\begin{Bmatrix} I_1 & I_1 & 1 \\ I_1 & I_1 & 1 \\ I & I'' & 2\end{Bmatrix}.$$

Here $F$ is the total angular momentum, $J$ is the total angular momentum apart from nuclear spin, $I_1$ is the spin of a single $^{23}$Na nucleus, and $I$ and $I''$ are values of total nuclear spin. The electric quadrupole, spin-rotation, scalar spin-spin, and tensor spin-spin coupling constants are denoted by $eqQ$, $c$, $\delta$, and $d$, respectively. Formulas for these constants will be discussed below.

Figure 1 shows the pattern of hyperfine levels in the $X^1\Sigma_g^+$ state for typical even- and odd-$J''$ states; the marked difference is due to the Pauli principle applied to the identical nuclei of spin $\frac{3}{2}$, which requires that states of even (odd) $J''$ be associated with total nuclear spin values of $I=0,2$ ($I=2,3$). The electric quadrupole and tensor spin-spin interactions mix levels with the same to-

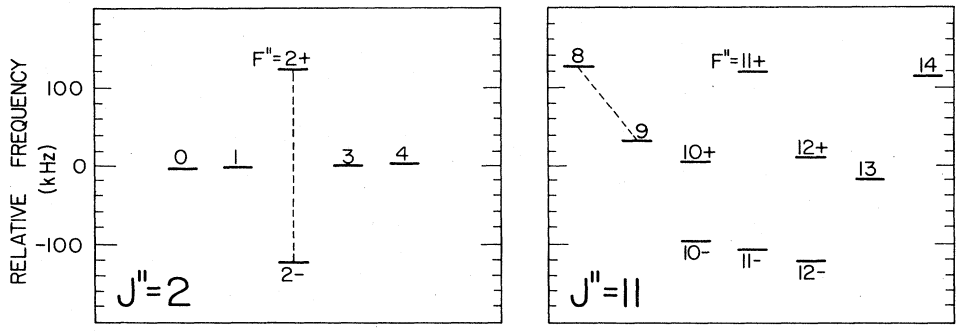


FIG. 1. Hyperfine energy levels for typical even- and odd-$J''$ rotational levels of the $X^1\Sigma_g^+$ state of $Na_2$. The dashed lines indicate coherence-free transitions used in this work.

tal angular momentum $F''$ and different $I$, giving pairs of levels labeled $F''+$ and $F''-$. Of the five transitions having frequencies greater than $\sim 100$ kHz in the $J''=2$ case, only the $2+\leftrightarrow 2-$ one is free of coherence effects because both of the levels involved are far from the other levels to which they could be optically coupled. By contrast, in the odd-$J''$ case it is possible to find several coherence-free transitions that are suitable for a determination of the hfs constants, although accidental blends often limit the possibilities.

### B. Optical pumping

The "optical-pumping cycle" in the molecular case is essentially a depletion process because spontaneous emission from the excited state is unlikely to repopulate the initial ground-state rotational-vibrational level. As discussed above, the coherence between ground-state sublevels produced by absorption and stimulated emission has a negligible effect on all the transitions studied here because of velocity averaging.

Parity considerations for the $A$-$X$ band allow only $\Delta J=\pm 1$ optical transitions ($P$ and $R$ branches), and the strongest hyperfine components will have $\Delta F=\Delta J$. Furthermore, if we choose the $z$ axis parallel to the laser electric field, only $\Delta M_F=0$ transitions are allowed. With $\Delta J=-1$ [a $P(J'')$ line] and the above selection rules, one finds that the ground-state magnetic sublevels with $|M_F|=F$ will have very low transition probabilities compared to all the others, and thus retain most of their original population. Figure 2(a) shows the magnetic sublevels of a pair of ground-state hyperfine levels $F$ and $F+1$ with an indication of their relative optical-absorption probabilities. The higher the absorption probability, the less population will remain after exposure to the laser in the $A$ region. The three possible hyperfine transitions emanating from the sublevel $(F, M_F=F)$ are denoted by $s_1$, $p$, and $s_2$, corresponding to $\Delta M_F=+1,0,-1$; their matrix elements for $F\gg 1$ are in the ratio $\sqrt{2F}:\sqrt{2F}:1$. Even though the $s_1$ matrix element is the largest, it connects two levels of nearly equal population, whereas the $p$ transition connects a level that retains almost its full original population with a nearly empty one. Thus for $F\gg 1$ we expect the signals for $p$-case laser polarization to be larger than those for the $s$ case. A corresponding examination of an $F+\leftrightarrow F-$ transition [Fig. 2(b)] shows that the $s$-case signals will be larger here; even though the $p$ matrix element is the largest (by a factor of $\approx\sqrt{F}$), the population difference for the $p$ transition is much smaller than for the $s$ transitions. This simple signal model also implies that the use of an $R$ line for optical pumping, instead of a $P$ line, will substantially deplete all $M_F$ levels, giving very small signal strength; this is in fact observed.

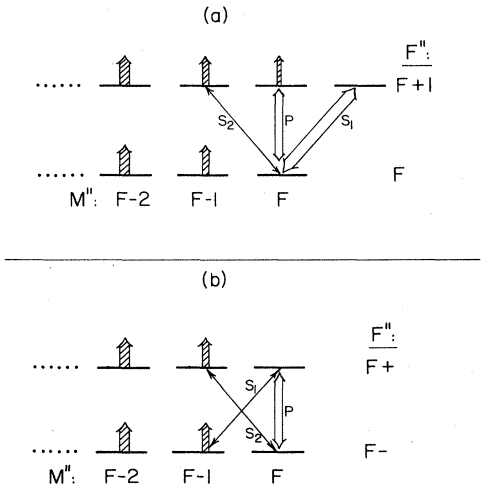


FIG. 2. Magnetic sublevels for pairs of hyperfine levels (a) $F''=F,F+1$ and (b) $F''=F+,F-$. The shaded arrows indicate allowed optical transitions to the $A^1\Sigma_u^+$ state (not shown). The arrows labeled $s_1,p,s_2$ represent rf transitions between hyperfine levels satisfying $\Delta M_F=+1,0,-1$, respectively. The widths of all arrows indicate qualitatively the relative transition probability. Note that the absence of vertical arrows from the $M_F=F$ levels indicates a very low transition probability.

## III. EXPERIMENT AND RESULTS

The apparatus for observing rf transitions between hyperfine levels has been described in Ref. 22. Briefly, a collimated, supersonic molecular beam containing a few percent $Na_2$ passes sequentially through three regions conventionally referred to as $A$, $C$, and $B$. In the $A$ region, a normally incident, linearly polarized laser tuned to a specific rotational line of the $A^1\Sigma_u^+\leftarrow X^1\Sigma_g^+$ system optically pumps the molecules to produce an alignment in the ground-state hyperfine levels. A rf magnetic field produced in a flattened solenoid (the $C$ region) drives hyperfine transitions with the selection rule $\Delta M_F=0$ or $\Delta M_F=\pm 1$, depending on the relative polarization of the laser and rf fields. Finally, the change in alignment caused by the rf field is monitored by observing the fluorescence produced at another laser—molecular-beam intersection (the $B$ region). The amplitude of the rf field is modulated at 107 Hz and the accompanying change in the laser-induced fluorescence is observed with a synchronously driven up-down counter.

The tunable cw standing-wave laser used for this work operated with Rhodamine 640 dye and was frequency-stabilized to either an iodine-absorption line or a temperature-stabilized confocal étalon, depending on which $Na_2$ rotational line was being studied. Typical single-mode power was a few milliwatts in a Gaussian beam with $1/e^2$ width $\sim 4.5$ mm at the $A$ and $B$ regions; the transit time in each of these regions was $\sim 3$ $\mu$s. For most of the higher-$J$ lines observed, the laser was polarized parallel to the rf magnetic field ($p$ case) rather than perpendicular to it ($s$ case) since this produced larger signals, as explained above. In the absence of coherence effects, the laser polarization should have no effect on the line position or shape.

A typical rf transition is shown in Fig. 3; it is symmetric and has a full width at half maximum (FWHM) of about 3 kHz, consistent with a 0.3-ms transit time through the $C$ region. The optical-pumping model discussed above suggests that each hyperfine transition (especially $p$-case transitions for not too small $J$ values) can be

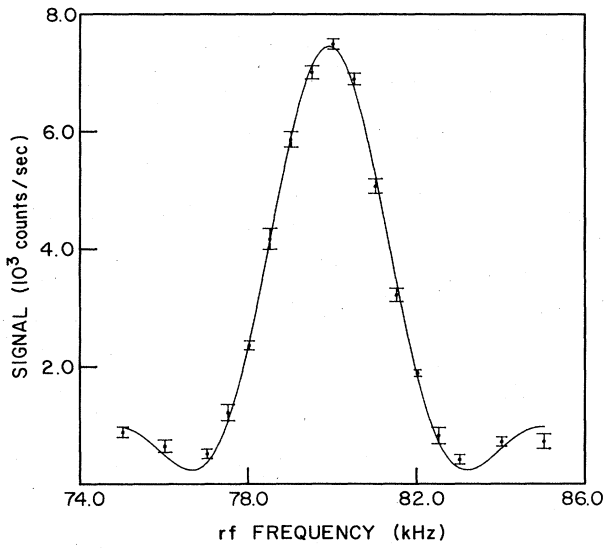


FIG. 3. The double-resonance signal for the hyperfine transition between the $F''=1$ and $F''=2+$ levels in the $J''=1$ rotational level of the $X$ state of $Na_2$. The fluorescence from the $Na_2$ beam in the $B$ region is plotted against the frequency of the rf magnetic field in the $C$ region. The curve is a velocity-averaged Rabi two-level line-shape fit to the data.

regarded approximately as a two-level case for which the transition matrix element $b$ can be easily calculated using the measured rf magnetic fields:

$$b=\frac{\mu_N}{2h}B(g_I\langle F_2M_F\,|\,I_k\,|\,F_1M_F\rangle + g_J\langle F_2M_F\,|\,J_k\,|\,F_1M_F\rangle)\,, \quad (1)$$

where $\mu_N$ is the nuclear magneton, $g_I$ and $g_J$ are the $g$ factors corresponding to the nuclear and rotational magnetic moments, and $B$ is the amplitude of the sinusoidal rf magnetic field in the $k$ direction. Accordingly, the center frequency was determined by fitting the data with a Rabi two-level line shape[26] averaged over the velocity distribution in the molecular beam. The center frequency, $b$ value, and overall amplitude of the signal were varied. Generally, this procedure gave a curve which fit very well over the central peak, but had subsidiary maxima which were too pronounced. This arises because the data represent (especially for low $J$) the superposition of transitions among several degenerate levels of different $M_F$: the FWHM of the Rabi line shape is not very sensitive to the value of $b$ for $bt<\pi/2$ (where $t$ is the time of flight in the $C$ region), while the positions and amplitudes of the subsidiary maxima do vary with $b$.

In general, the fitted $b$ values were in reasonable agreement ($\approx$20%) with values calculated from Eq. (1) using the measured rf current in the coil and the appropriate $s_1$ or $p$ matrix elements. The agreement in the $s_1$ case suggests that the ratio of the $s_1$ to $s_2$ matrix elements is large enough to overcome the population-difference advantage of the $s_2$ transition. In a few cases, the fit amplitude and $b$ values were physically unreasonable; the addition of a background parameter rectified this without producing any significant change in the center frequency. It should be emphasized that the values of the center frequencies are quite insensitive to the detailed nature of the fit curve; even a cubic spline interpolation did not shift the values by amounts significant at our level of precision.

In all, some 30 lines were measured in rotational levels with $J''=1$–29. Rejection of a few noticeably asymmetric blended lines left 24 for a least-squares determination of the hyperfine constants. Table I gives the measured and fit frequencies for each of the 24 lines included in the fit. The errors on the measured frequencies are derived from the Rabi line-shape fit. All but two of the lines belong to rotational levels of odd $J''$ for reasons given above; the remaining two are $F''=J''+\leftrightarrow F''=J''-$ transitions. In the $J''=1$ case, *all* of the seven possible transitions were observed; this allows an immediate consistency check, since some frequencies are sums of two others (see Fig. 4); the agreement is at the two-standard-deviation level. The fit included the four hyperfine constants $eqQ$, $c$, $d$, and $\delta$; to take into account centrifugal effects, $eqQ$ was written as $eqQ_0+\beta J(J+1)$, thus introducing a fifth constant. Experimenting with the fit showed that $\beta$ was in fact determined, while analogous coefficients for the other hyperfine constants were zero to the precision of the data. Because the reduced $\chi^2$ of 5.0 was rather large (due primarily to two points), the possibility of additional hyperfine interactions was considered. Broyer *et al.*[25] raise the possibility of observing *second-order* quadrupole interactions in the hyperfine spectrum of $I_2$; barring fortuitous cancellations in the perturbation theory sum, this would imply that off-diagonal electric

TABLE I. Measured and fitted hyperfine transition frequencies (kHz). (Diff. denotes difference.)

| $J$ | $(F_1,F_2)$ | $\nu_{\text{data}}$ | $\nu_{\text{fit}}$ | Diff. |
|---|---|---|---|---|
| 1 | (0,1) | 274.214(127) | 274.097 | −0.117 |
| 1 | (1,2-) | 164.896(16) | 164.810 | −0.086 |
| 1 | (1,2+) | 79.904(16) | 79.887 | −0.017 |
| 1 | (2+,2-) | 244.752(29) | 244.697 | −0.055 |
| 1 | (2-,3) | 59.684(29) | 59.657 | −0.027 |
| 1 | (2+,3) | 304.340(26) | 304.354 | 0.014 |
| 1 | (3,4) | 185.684(25) | 185.659 | −0.025 |
| 2 | (2+,2-) | 244.268(20) | 244.399 | 0.131 |
| 3 | (4,5) | 89.401(21) | 89.407 | 0.006 |
| 5 | (8,7) | 144.098(42) | 144.073 | −0.025 |
| 7 | (5,6) | 43.615(238) | 43.822 | 0.207 |
| 7 | (8,9) | 39.865(137) | 39.923 | 0.058 |
| 7 | (9,10) | 138.378(33) | 138.344 | −0.034 |
| 11 | (8,9) | 96.830(100) | 96.957 | 0.127 |
| 13 | (10,11) | 99.185(41) | 99.195 | 0.010 |
| 15 | (12,13) | 100.744(22) | 100.720 | −0.024 |
| 15 | (17,18) | 130.750(50) | 130.767 | 0.017 |
| 17 | (14,15) | 101.757(30) | 101.796 | 0.039 |
| 17 | (19,20) | 130.189(32) | 130.244 | 0.055 |
| 19 | (16,17) | 102.443(101) | 102.574 | 0.131 |
| 19 | (21,22) | 129.979(56) | 129.957 | −0.022 |
| 21 | (18,19) | 103.138(28) | 103.145 | 0.007 |
| 28 | (28+,28-) | 231.700(60) | 231.654 | −0.046 |
| 29 | (31,32) | 130.588(73) | 130.535 | −0.053 |

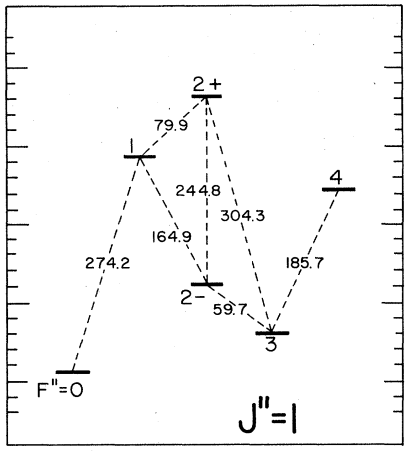


FIG. 4. Hyperfine energy levels and observed rf transitions for the $J''=1$ rotational level of the $X$ state of $Na_2$. The measured frequencies are shown in kHz.

quadrupole matrix elements are comparable to the off-diagonal magnetic dipole matrix elements that contribute to $c$, $d$, and $\delta$. Even though this is not the case for $Na_2$, we added the terms in $e$, $f$, and $h$ to the hfs model (see Ref. 25, Table V a). The reduced $\chi^2$ was somewhat larger and the constants $e$, $f$, and $h$ were all consistent with zero values, while the values of the five nonzero constants did not change by statistically significant amounts. The values of these five constants, as derived from a fit with $e$, $f$, and $h$ set to zero, are given in Table II.

## IV. DISCUSSION AND CONCLUSIONS

In the case of the hyperfine constants $eqQ$ and $c$, a comparison can be made with earlier results. Using the values of $eqQ_0$ and $\beta$ from this work gives $eqQ=-464.89(21)$ kHz for $J''=28$, which is in good agreement with our previous value of $-463.70(90)$ kHz.[20] Our previous estimate of the absolute value of the spin-rotation constant $c$ does not agree as well with the present value. The old value was based on two independent methods, which did not agree with each other. The value believed to be more reliable was derived from the frequency separation of two partially resolved peaks in the $J''=28$ rf spectrum; each of these peaks is itself an unresolved blend of two lines. Furthermore, the spectrum in question was observed in the $s$-polarization case, which subsequent work[22,23] has shown was distorted due to coherence effects. Interestingly enough, the inclusion of the spin-spin interaction in the Hamiltonian used at that time would not have affected the value of $c$ significantly: the energy-level difference corresponding to the observed peak separation is quite insensitive to the spin-spin interaction.

TABLE II. hfs coupling constants for $Na_2$ $X^1\Sigma_g^+$, $v''=0$, from a least-squares fit.

| | |
|---|---|
| Electric quadrupole: | $eqQ=[-458.98(4)$ $-0.007\,28(25)J(J+1)]$ kHz |
| Nuclear spin-rotation: | $c=242.9(1.5)$ Hz |
| Tensor spin-spin: | $d=302.6(5.0)$ Hz |
| Scalar spin-spin: | $\delta=1066.7(6.5)$ Hz |

A comparison of the measured hyperfine constants with *ab initio* calculations is a formidable task since all of the constants involve reduced matrix elements requiring electronic wave functions for the molecule. The presence of significant second-order contributions implies that wave functions and energies for excited electronic states are also required. In the case of constants representing, at least in part, a direct interaction between the two nuclei, there is a first-order term depending on the expectation value of some power of the internuclear separation, $r_{12}$, which can easily be estimated.

The first-order contribution to the spin-rotation constant $c$ corresponds to the spin-orbit interaction between the two nuclei *shielded by their core electrons*

$$c_D=-\frac{\mu_0}{4\pi}\frac{4\mu_n^2 g_I}{h}\frac{Z_{\text{eff}}}{M}\langle r_{12}^{-3}\rangle \text{ Hz},$$

where $Z_{\text{eff}}$ is the atomic number minus the number of electrons in closed shells around the nucleus, $\mu_n$ is the nuclear magneton, and $M$ is the nuclear mass in atomic mass units. Taking $Z_{\text{eff}}=1$ and $\langle r_{12}^{-3}\rangle=(3.079\times10^{-10}\text{ m})^{-3}$ gives $c_D=-34$ Hz. The experimental result for $c$ is 242.9(1.5) Hz, implying a second-order contribution of $\sim277$ Hz. This second-order term, denoted $c_E$, arises from the cross term involving the magnetic dipolar interaction $H_{\text{MD}}$ between the nuclei and the electrons, and the off-diagonal part, $V$, of the molecular Hamiltonian, which is independent of $I$ (the rotation-electronic and electron spin-orbit terms).[25] Since $V$ has no matrix elements between $g$ and $u$ electronic states, the perturbing states for a $^1\Sigma_g^+$ ground state must be $\Pi_g$ in character. A candidate is a $C^1\Pi_g$ state predicted to lie 20 815 $\text{cm}^{-1}$ above the ground state. Two fairly crude methods for estimating $c_E$ are given in the Appendix; they give 46 and 256 Hz, which are at least of the right order of magnitude.

The spin-spin interaction between the two nuclei also consists of first- and second-order parts (to the same order of approximation). The Hamiltonian for the first-order part is just the classical dipole-dipole interaction, which can be written in terms of rank-2 spherical tensors. The coupling constant $d_D$ is given by[25]

$$d_D=\frac{\mu_0}{4\pi}(g_I\mu_n)^2\langle v=0\,|\,r_{12}^{-3}\,|\,v=0\rangle,$$

which yields 288 Hz. In second order, $H_{\text{MD}}$ contributes a rank-2 tensor part with a coupling constant $d_E$ and identical dependence on the angular momentum quantum numbers, so that the measured coupling constant corresponds to $d_D+d_E$. The experimental value $d=302.6(5.0)$ Hz and the calculated $d_D$ thus imply that $d_E=15(5)$ Hz.

Taken to second order, $H_{\text{MD}}$ also contributes to the effective Hamiltonian a scalar term $\delta\mathbf{I}_1\cdot\mathbf{I}_2$. Because the terms in $d_E$ and $\delta$ arise from the same operator in second order, they have very similar formulas involving the usual sum over excited electronic states. In fact, if one excited

state dominates the sum, the ratio $d_E/\delta$ will be a simple fraction of the order of unity. Our experimental value for $\delta$ is 1066.7(6.5) Hz, which is much larger than the derived value for $d_E$. A situation like this can arise when more than one electronic state makes a significant contribution to the perturbation sum. In the case at hand, suppose the states $A\,^1\Sigma_u^+$ and $B\,^1\Pi_u$ are the only important ones. (A positive value for $\delta$ implies that perturbing states of $u$ character are dominant here.) The formulas[25] for $d_E$ and $\delta$ show that $d_E/\delta=-1$ for the $A$-state term, and $\frac{1}{2}$ for the $B$-state term. Thus we can write that

$$\delta\approx 2B+2A \quad \text{and} \quad d_E\approx B-2A \ ,$$

where $A$ and $B$ are two positive constants which depend on reduced matrix elements and energy denominators. In such a situation, $d_E$ could thus be much smaller than $\delta$, as we have observed.

In conclusion, we have observed many hyperfine transitions in several rotational levels of the $v''=0$, $X\,^1\Sigma_g^+$ state of $Na_2$. Twenty-four of these transitions, with line shapes believed to be free of distortion by coherence effects, have been fitted with five constants; the values for $\beta$, $d$, and $\delta$ represent first-time measurements. A reexamination of models of coherent line shapes is underway in the light of these new values for the hyperfine constants. Early results are encouraging in that some nagging discrepancies between experiment and theory are resolved using the new values. The completed study will be published at a later date.[23]

## APPENDIX

Here we present two rough estimates of $c_E$, the electron-coupled part of the nuclear spin-rotation coupling constant. The first depends on a connection between $c_E$ and the electronic contribution $g_J^e$ to the molecular $g$ factor. It can be shown[27] that if one low-lying excited electronic state dominates the second-order perturbation sum on which both quantities depend, then

$$c_E\approx -\left[\frac{\mu_0}{4\pi}\right]2g_J^e g_I\mu_N^2\langle r^{-3}\rangle_{0n} \ ,$$

where $\mu_N$ is the nuclear magneton, $g_I$ is the nuclear $g$ factor, and $r$ is the distance between the excited-state valence electron and a nucleus. The quantity $\langle r^{-3}\rangle_{0n}$ is an off-diagonal matrix element between the ground and excited electronic states; in rough estimates, it is common[27,28] to approximate it by one-half the expectation of $r^{-3}$ in the excited *atomic* state, which corresponds most closely to the excited molecular state. Since the excited state must be of $\Pi_g$ character, we consider a $C\,^1\Pi_g$ state[15] whose dominant configuration involves an excited $\pi_g$ electron, which is asymptotically an atomic $3p$ orbital. Using[29] $\langle r^{-3}\rangle_{3p}=0.244(a_0)^{-3}$ and[19] $g_J^e=-0.004\,90$ gives $c_E=46$ Hz.

In the second method, we consider the second-order formula for $c_E$, again in the approximation that one excited electronic state dominates the sum:

$$c_E\approx 8g_I\mu_N\mu_B B\langle r^{-3}\rangle_{0n}\frac{|\langle 0|L_x|n\rangle|^2}{E_n-E_0} \ ,$$

where $B$ is the rotational constant, $\mu_B$ is the Bohr magneton, and $L_x$ is the component of electronic orbital angular momentum perpendicular to the internuclear axis. The state 0 is the ground electronic state, and $n$ again represents the $C\,^1\Pi_g$ state whose energy is calculated to be 20 815 $cm^{-1}$ above the ground state. In the "pure precession" approximation of Van Vleck,[30]

$$|\langle 0|L_x|n\rangle|^2=l(l+1)/4 \ ,$$

where $l=1$ here for the $p$ electron. Using the same estimate of $\langle r^{-3}\rangle_{0n}$ as before yields $c_E=256$ Hz.


[1]W. Demtröder, M. McClintock, and R. N. Zare, J. Chem. Phys. **51**, 5495 (1969).

[2]K. K. Verma, J. T. Bahns, A. R. Rajaei-Rizi, and W. C. Stwalley, J. Chem. Phys. **78**, 3599 (1983). This work contains a comprehensive bibliography for the $Na_2$ molecule.

[3]P. Kusch and M. M. Hessel, J. Chem. Phys. **63**, 4087 (1975).

[4]H. Itoh, M. Hayakawa, Y. Fukuda, and M. Matsuoka, Opt. Commun. **36**, 131 (1981).

[5]M. E. Kaminsky, J. Chem. Phys. **66**, 4951 (1977); **73**, 3520 (1980).

[6]W. Demtröder and M. Stock, J. Mol. Spectrosc. **55**, 476 (1975).

[7]P. Kusch and M. M. Hessel, J. Chem. Phys. **68**, 2591 (1978).

[8]K. K. Verma, T. H. Vu, and W. C. Stwalley, J. Mol. Spectrosc. **91**, 325 (1982).

[9]N. W. Carlson, A. J. Taylor, and A. L. Schawlow, Phys. Rev. Lett. **45**, 18 (1980).

[10]A. J. Taylor, K. M. Jones, and A. L. Schawlow, Opt. Commun. **39**, 47 (1981).

[11]T. W. Ducas, M. G. Littman, M. L. Zimmerman, and D. Kleppner, J. Chem. Phys. **65**, 842 (1976).

[12]W. Demtröder, W. Stetzenbach, M. Stock, and J. Witt, J. Mol. Spectrosc. **61**, 382 (1976).

[13]P. Kusch and M. M. Hessel, J. Chem. Phys. **63**, 4087 (1975).

[14]J. B. Atkinson, J. Becker, and W. Demtröder, Chem. Phys. Lett. **87**, 92 (1982).

[15]D. D. Konowalow, M. E. Rosenkrantz, and M. L. Olson, J. Chem. Phys. **72**, 2612 (1980).

[16]A. Valance and Q. N. Tuan, J. Phys. B **15**, 17 (1982).

[17]W. J. Stevens, M. M. Hessel, P. J. Bertoncini, and A. C. Wahl, J. Chem. Phys. **66**, 1477 (1977).

[18]R. A. Logan, R. E. Coté, and P. Kusch, Phys. Rev. **86**, 280 (1952).

[19]R. A. Brooks, C. H. Anderson, and N. F. Ramsey, Phys. Rev. **136**, 62 (1964).

[20]S. D. Rosner, R. A. Holt, and T. D. Gaily, Phys. Rev. Lett. **35**, 785 (1975).

[21]R. Huber, F. König, and H. G. Weber, Z. Phys. A **281**, 25 (1977).

[22]A. G. Adam, S. D. Rosner, T. D. Gaily, and R. A. Holt, Phys. Rev. A **26**, 315 (1982).

[23]R. A. McLean, T. D. Gaily, R. A. Holt, and S. D. Rosner (unpublished).

[24]R. A. Frosch and H. M. Foley, Phys. Rev. **88**, 1337 (1952).
[25]M. Broyer, J. Vigué, and J. C. Lehmann, J. Phys. (Paris) **39**, 591 (1978).
[26]N. F. Ramsey, *Molecular Beams* (Oxford University Press, London, 1955).
[27]C. H. Townes and A. L. Schawlow, *Microwave Spectroscopy* (Dover, New York, 1975), Chap. 8.
[28]R. L. White, Rev. Mod. Phys. **27**, 276 (1955).
[29]R. G. Barnes and W. V. Smith, Phys. Rev. **93**, 95 (1954).
[30]J. H. Van Vleck, Phys. Rev. **33**, 467 (1929).